

Modeling high burnup structure in oxide fuels for application to fuel performance codes. Part II: Porosity evolution

Tommaso Barani^{a,1}, Davide Pizzocri^a, Fabiola Cappia^b, Giovanni Pastore^c, Lelio Luzzi^a, Paul Van Uffelen^{d,*}

^a Politecnico di Milano, Department of Energy, Nuclear Engineering Division, via La Masa 34, Milano I-20156, Italy

^b Idaho National Laboratory, Idaho Falls, ID 83415, USA

^c Department of Nuclear Engineering, University of Tennessee, Knoxville, TN 37916, USA

^d European Commission, Joint Research Centre (JRC), Karlsruhe, Germany



ARTICLE INFO

Article history:

Received 13 December 2021

Revised 5 February 2022

Accepted 25 February 2022

Available online 4 March 2022

Keywords:

High burnup structure

Porosity

Oxide fuel

Fission gas behaviour

Fuel performance codes

ABSTRACT

We propose a model describing the high burnup structure inter-granular porosity evolution under irradiation. The evolution of the porosity collecting the gas diffusing from the grains is modeled by exploiting a second-order Fokker-Planck expansion of the cluster-dynamics master equations governing the problem, considering nucleation of pores, gas absorption due to the diffusional flow from the grains, size-dependent re-solution of gas from pores due to interaction with fission fragments, vacancy absorption, and pore coalescence. Model predictions on xenon local retention, matrix fuel swelling, and porosity evolution are compared to experimental data and to models available in fuel performance codes.

© 2022 The Authors. Published by Elsevier B.V.

This is an open access article under the CC BY license (<http://creativecommons.org/licenses/by/4.0/>)

1. Introduction

As the conditions for the formation of the high burnup structure (HBS) are attained (i.e., local burnups above 45/50 MWd kg⁻¹ and local temperatures below 1000 °C), the formation of a novel porosity is observed in the fuel [1,2]. With the absorption of fission gas diffusing to grain boundaries as the fuel grains in the HBS undergo gas depletion [3–5], the porosity evolves up to causing significant local swellings [1,2]. Given the important consequences brought by the presence of a high porosity region in the fuel (on e.g., its thermal performance, its mechanical interaction with the cladding, its retention properties, and its ability to withstand thermal transients), it is necessary to develop models to equip fuel performance codes with reliable predictive capabilities for HBS porosity evolution.

Jernkvist [6] adopted the concept proposed by Lassmann [7] to describe xenon depletion, while the development of HBS porosity was tackled assuming dislocation punching as the driving force,

and is described through a simple and pragmatic growth equation governed by the pore pressure difference with respect to an empirical pressure threshold. The model has been made available to the FRAPCON/FRAPTRAN codes [8]. Lemes et al. [9] extended the model by Lassmann, including the treatment of Kr and complementing it with a mixed empirical and mechanistic description of the porosity development. As for the porosity evolution, the model is a combination of empirical correlations and of the model by Blair and co-workers [10] for considering pore interactions for local burnups exceeding 100 MWd kg⁻¹. The model is implemented in the DIONISIO code [11].

The model by Khvostov and coworkers [12,13] pairs a semi-empirical treatment of HBS formation to a description of pore evolution at grain boundaries. There, the gas diffused from the grains can be accommodated in existing pores – or create new ones – contributing to pore growth together with the trapping of point defects. To this aim, the model considers an empirical reduction of the grain size, dependent on the local burnup and temperature, and an empirical but unspecified increase of the effective volumetric vacancy diffusion dependent amongst others on the local degree of restructuring. Finally, pore coalescence based on probabilistic considerations and a-thermal fission gas release mechanisms are accounted for. The overall model is grafted in the GRSW-A model [13] and integrated in the FALCON code [14].

* Corresponding author.

E-mail addresses: tommaso.barani@cea.fr (T. Barani), davide.pizzocri@polimi.it (D. Pizzocri), fabiola.cappia@inl.gov (F. Cappia), gpastore@utk.edu (G. Pastore), lelio.luzzi@polimi.it (L. Luzzi), paul.van-uffelen@ec.europa.eu (P. Van Uffelen).

¹ Current address: Commissariat à l'Énergie Atomique et aux Énergies Alternatives, DES/IRESNE/DEC/SESC, Saint-Paul-lez-Durance Cedex, 13108, France.

L. Noirot proposed a comprehensive model for the evolution of HBS [15]. In this model, the porosity evolution is tackled considering a number of nucleated pores proportional to the degree of local restructuring, and ascribing pore growth to the absorption of gas diffused from the restructured grains and to vacancy inflow driven by pore over-pressurization. The phenomena are modeled by the classic formalism of diffusion-limited reactions in the mean-field approximation. No pore interconnection is considered in the model, whereas a multiplication factor enhancing vacancy diffusivity, similarly to the work by Blair and coauthors [10], is considered. The description is plugged in the MARGARET code, which provides a mechanistic description of fission gas behavior, and is integrated into the ALCYONE code [16,17].

Kremer and coauthors [18] proposed an empirical approach to model HBS porosity in the MFPR/F code. They coupled a mechanistic description of HBS formation and intragranular bubble behavior to an empirical correlation based on the local porosity data by Cappia and coauthors [2] as a function of burnup in the MFPR/F code.

Besides the aforementioned empirical and semi-empirical models, more mechanistic models have been developed to describe HBS porosity. Rest [19,20] proposed a comprehensive, mechanistic description of HBS formation and porosity evolution, based on the rate theory approach. Veshchunov and Shestak [21] proposed a model accounting for the evolution of point, line, and volume defects under irradiation. The key parameter determining HBS formation is the predicted dislocation density, which is compared to a threshold inferred from experimental data [22] to establish HBS formation. Albeit featuring a consistent description of defects evolution, the transition from original to restructured microstructure is step-wise, thus likely failing to properly describe the gradual xenon depletion experimentally observed. Moreover, the assumption of mean-field concentration of vacancies and interstitials might be questionable when applied to HBS, due to high local concentrations of defects and sinks [23]. Furthermore, the evolution of HBS porosity is grafted in a more general model holding for UO_2 porosity evolution under different conditions [24], and considers the pore interaction with vacancies and gas atoms diffusing from the grains. Yet, the growth of pores is ascribed to vacancy precipitation and was the object of further publications [24–26]. In the latest work [26], however, the authors propose dislocation punching as the leading mechanism for pore growth at high burnups. Moreover, they account for the pore coarsening observed at ultra high burnups via a triple collision interconnection model, considering a polydispersed pore distribution. The model is available in the MFPR/R code [27], which is included in the SFPR and BERKUT codes [28].

In a companion paper [29], we proposed a novel model describing HBS formation and intra-granular xenon depletion. The HBS formation – i.e., the increase of local fuel volume that underwent restructuring as a function of the local effective burnup – is described through the KJMA formalism for phase transitions [30,31]. The HBS formation is paired to a mechanistic model describing intra-granular fission gas behavior [29], providing the evolution under irradiation of the intra-granular bubble population, accounting for bubble nucleation, gas atom trapping into and irradiation-induced re-solution from bubbles, along with diffusion of gas atoms to the grain boundaries. Estimating the evolving concentrations of retained gas into the grain allows us to consistently calculate the fuel matrix swelling, i.e., the swelling due to solid fission products and to inert fission gas atoms found in the fuel matrix and in intra-granular bubbles, up to high burnups. In this work, we add modeling the evolution of the HBS inter-granular porosity, which is tackled considering a Fokker-Planck approximation of the master equations governing the gas evolution at grain boundaries. The Fokker-Planck expansion yields a model featured by a limited number of equations, tracking the evolution of pore average size,

pore-distribution variance, and pore number density, yet considering in a mechanistic fashion the phenomena determining pore evolution, i.e., irradiation-driven re-solution and gas trapping. Because the pores are generally over-pressurized, we consider the vacancy absorption by the pores as a further mechanism of growth, together with the coalescence of immobile pores by interconnection and impingement. We implemented the model in the stand-alone, open-source, meso-scale computer code SCIANTIX [32], which has been coupled with the TRANSURANUS code [33].

We present the stand-alone validation of model predictions, by comparing the model predictions in terms of pore number density, average radius, and resulting swelling to the experimental data by Spino and co-workers [1] and Cappia and co-workers [2], as well as to models available in fuel performance codes (FPCs) and to the model presented by Kremer et al. [18] available in MFPR/F, which has also been coupled with TRANSURANUS. The comparison to more complex models, e.g., the model by Veshchunov and co-workers available in the MFPR/R code [21,25,26], is of interest in perspective to further assess the modeling framework proposed in this work. The comparison will be the subject of a future work centered on a thorough and systematic comparison between the simulations results and models of SCIANTIX and MFPR/F.

The proposed description of HBS porosity, whose foundations lie on the master equations of cluster dynamics, allows for including the effects due to the pore size distribution on the trapping and re-solution rates. This constitutes a step forward with respect to the available single-size models [10,13,15,19,24] in both fidelity of the physical description and the resulting transferability of the model to different operating conditions, such as consideration of the pore size for fragmentation during LOCA as suggested by Kulacsy [34]. These aspects are combined to the required characteristics for models included in engineering-scale fuel performance codes used for industrial and research purposes, i.e., an acceptable computational burden and an optimal numerical stability.

2. Formulation of the model for high burnup structure porosity evolution

In this Section, we present the derivation of a model describing the evolution of inter-granular porosity in the HBS. The model is derived starting from the cluster dynamics master equations governing the inter-granular gas behavior, enforcing a Fokker-Planck expansion in the phase space of the problem (i.e., cluster sizes) to come up with a model tracking the evolution of the three first central moments, i.e., integral pore number density, mean pore size and variance of the size-distribution. On top of this, vacancy absorption due to pore over-pressurization and pore interconnection by impingement are accounted for and integrated. Together with the HBS formation and intra-granular model presented in the companion paper [29], this model provides an integral description of fission gas behavior in the HBS, ready to be included in FPCs.

2.1. Fokker-Planck approximation of CD master equations

In order to describe the evolution of HBS pores, we employ a cell model (e.g., [35,36]), i.e., a regular 3D array of spherical Wigner-Seitz cells is associated to the pore pattern. A 2D sketch of the representation is provided in Fig. 1(a).

The evolution of HBS pores is described by the master equations of cluster dynamics (e.g., [37–39]) which accounts for the phenomena of pore nucleation, re-solution, gas precipitation from the grain boundaries – as sketched in Fig. 1(b). In the following, we assume that re-solution events lead to the destruction of the pore (i.e., an *heterogeneous* re-solution modeling approach). The formu-

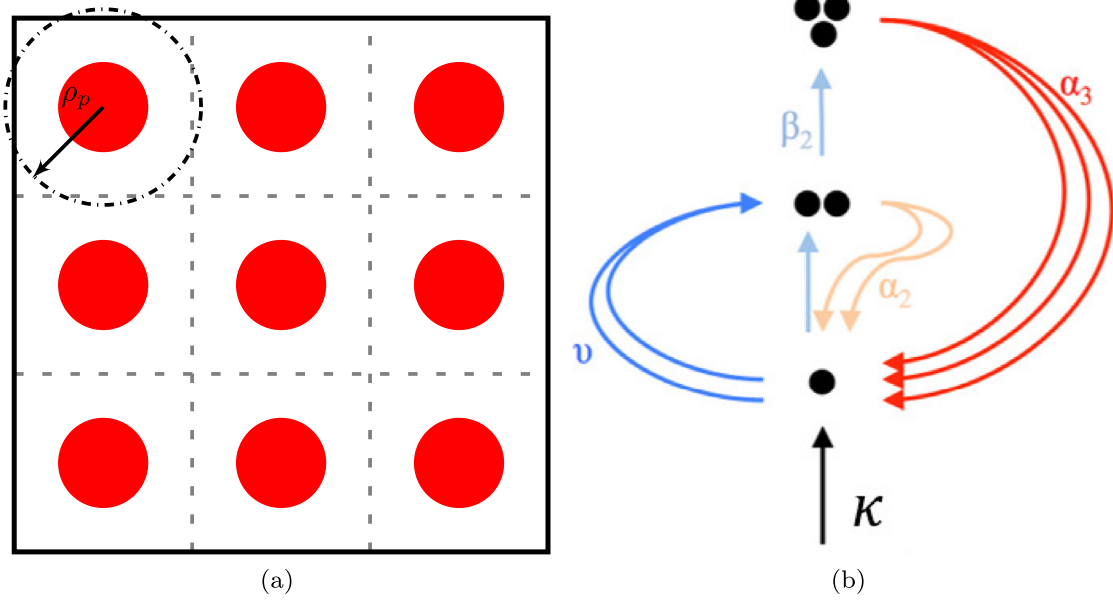


Fig. 1. Left: sketch of the model employed in this work to represent HBS pore growth, based on [36]. Right: Schematization of the phenomena accounted by the CD master equations.

lation of the master equations reads

$$\begin{cases} \frac{\partial c_{gb}}{\partial t} = \kappa - 2\nu_p - \sum_{n=2}^{\infty} \beta_n c_n + \sum_{n=2}^{\infty} n\alpha_n c_n \\ \frac{\partial c_2}{\partial t} = \nu_p - \alpha_2 c_2 \\ \frac{\partial c_3}{\partial t} = \beta_2 c_2 - \alpha_3 c_3 \\ \vdots \\ \frac{\partial c_n}{\partial t} = \beta_{n-1} c_{n-1} - \alpha_n c_n \end{cases} \quad (1)$$

where c_{gb} (at m^{-3}) is the gas concentration at the grain boundaries not trapped in pores, c_2, c_3, \dots, c_n (at m^{-3}) are the number density of pores containing 2,3,...,n atoms, κ (at $m^{-3} s^{-1}$) is the gas arrival rate from the interior of the grains, ν_p (pores $m^{-3} s^{-1}$) is the pore nucleation rate, β_n and α_n (s^{-1}) represent the probability of gas precipitation into and re-resolution from HBS pores, respectively. The expression of the HBS pore re-resolution rate is taken from Veshchunov and Tarasov [40] and considers a size-dependent process, namely

$$\alpha_n = 2 \cdot 10^{-23} \dot{F} \left(\frac{3d_v}{3d_v + R_n^p} \right) \left(\frac{\delta_v}{\delta_v + R_n^p} \right) \quad (2)$$

where R_n^p (m) is the radius of a cluster (pore) containing n atoms, d_v (m) is the critical distance from the pore surface within which atom re-resolution occurs, and δ_v (m) is thickness of the re-resolution layer around the pore. It should be noticed that the present model does not consider a re-resolution back into the grains of the gas atoms ejected from HBS pores. While this assumption might be questionable when considering standard grain size fuel, HBS fuel is featured by such small (i.e., hundreds of nanometers) grains that the gas atoms would be dissolved very close to the grain boundaries. We consider diffusion of those gas atoms back to the grain boundaries as instantaneous.

Following Gosèle [23], we evaluated the precipitation rate of gas atoms from the grain boundaries into the pores

$$\beta_n = 4\pi D_{gb}^{SA} c_{gb} R_n^p (1 + 1.8\xi^{1.3}) \quad (3)$$

being D_{gb}^{SA} ($m^2 s^{-1}$) the grain-boundary diffusivity of single gas atoms. The original formulation by Ham [41] was corrected by Gösele [23] to account for the competitions between sinks on the precipitation rate. In fact, the local porosity ξ (/) – considering spherical pores – is evaluated as

$$\xi = \frac{4\pi}{3} N_p (R_n^p)^3 \quad (4)$$

where the total number density of pores, N_p (pores m^{-3}), is defined as

$$N_p = \sum_{n=2}^{\infty} c_n \quad (5)$$

and R_n^p is the number-averaged radius of the distribution. As for the nucleation rate, ν_p (pore $m^{-3} s^{-1}$), in the light of the large uncertainties associated to this parameter (e.g., [42,43]), we chose not to model it explicitly. Rather, we consider it as proportional to the local restructuring rate² as

$$\nu_p = 5 \cdot 10^{17} \frac{d\alpha_r}{dbu_{eff}} \quad (6)$$

where the proportionality constant is a model parameter. Finally, given the appreciable shift in the tilt angle of grain boundaries observed during the HBS formation [44,45] – which can be ascribed to primary recrystallization [46–48] – we introduce a preliminary modification of the diffusion coefficient of gas atoms (and vacancies) at grain boundaries with respect to that in pristine fuel. Based on the information extracted from the experimental work of Gercazak and co-workers [44], and considering the dependence of the grain boundary diffusion coefficient on the tilt angle proposed by Peterson [49], we propose the following correction for the grain boundary diffusion coefficient of atoms and vacancies

$$D' = D'(T) \cdot \frac{\sin[4^\circ \cdot (1 - \alpha_r) + 40^\circ \cdot \alpha_r]}{\sin(4^\circ)} \quad (7)$$

² As restructuring rate, we assume the derivative of the restructured volume fraction $\alpha_r = 1 - \exp(-2.77 \cdot 10^{-7} (bu_{eff})^{3.54})$ with respect to the local effective burnup, i.e., $\frac{d\alpha_r}{dbu_{eff}} = 3.54 \cdot 2.77 \cdot 10^{-7} (1 - \alpha_r) (bu_{eff})^{2.54}$. The exponent of the effective burnup was mistakenly reported in [29] as 3.35 instead of 3.54

where $D'(T)$ ($\text{m}^2 \text{s}^{-1}$) is the gas atom or vacancy diffusion coefficient at the grain boundaries, α_r ($/$) is the local fraction of restructured volume, and the correction term considers a weighted average between the average tilt angle observed in the non-restructured region (i.e., 4°) and the average tilt angle observed in the fully restructured region (i.e., 40°). This modification allows for an enhanced diffusivity of species at grain boundaries and the correction factor spans between 1 and about 10, at beginning and end of restructuring, respectively. The modification is consistent with the conclusions of the analyses on gas behavior in the HBS by Baron and co-workers [50] and by Blair and co-workers [10], although they proposed an empirical enhancement of the diffusivity about two and four orders of magnitude, respectively.

Since the solution of Eq. (1) is unpractical for application to FPCs [37,38], we focus on the evolution of the first three central moments of the cluster distribution instead of solving the set of (hundreds of) thousands of coupled equations given by 1. In particular, in addition to the integral of the pore size distribution, N_p , we consider the following two quantities

$$\begin{aligned} A &= \sum_{n=2}^{\infty} c_n n \\ B &= \sum_{n=2}^{\infty} c_n (n - \bar{n})^2 \end{aligned} \quad (8)$$

which are related to the mean and variance of the pore size distribution, \bar{n} (atom/pore) and M^2 (atom²/pore), by

$$\begin{aligned} \bar{n} &= \frac{A}{N_p} \\ M^2 &= \frac{B}{N_p} \end{aligned} \quad (9)$$

To express the time evolution of the quantities appearing in Eq. (8) and following Clement and Wood [37], we consider a second order Fokker-Planck expansion of the coefficients of Eq. (1) in the phase space of the problem, i.e., with respect to the cluster size, reading

$$\begin{aligned} \alpha_n &\approx \alpha(\bar{n}) + \left. \frac{\partial \alpha_n}{\partial n} \right|_{\bar{n}} (n - \bar{n}) + \frac{1}{2} \left. \frac{\partial^2 \alpha_n}{\partial n^2} \right|_{\bar{n}} (n - \bar{n})^2 \\ \beta_n &\approx \beta(\bar{n}) + \left. \frac{\partial \beta_n}{\partial n} \right|_{\bar{n}} (n - \bar{n}) + \frac{1}{2} \left. \frac{\partial^2 \beta_n}{\partial n^2} \right|_{\bar{n}} (n - \bar{n})^2 \end{aligned} \quad (10)$$

Combining Eqs. (1), (8), and (10), one obtains the following simplified model, able to estimate the evolution of the distribution (number-averaged) mean size and variance, together with pore number density and gas stored at grain boundaries³

$$\begin{cases} \frac{dN_p}{dt} = \nu_p - \alpha_{\bar{n}} N_p - \frac{1}{2} \alpha'' B \\ \frac{dA}{dt} = 2\nu_p + \beta_{\bar{n}} N_p - \alpha_{\bar{n}} N_p - \alpha' B + B \left(\frac{\beta''}{2} + \bar{n} \alpha'' \right) + \frac{\bar{n}^2}{2} \alpha'' A \\ \frac{dB}{dt} = \beta_{\bar{n}} N_p - \alpha_{\bar{n}} N_p + B(2\beta' + 3\alpha' \bar{n}) - 3\bar{n} B(\beta'' + \alpha'') + \frac{B}{2} (1 - 2\bar{n}) \beta'' - \bar{n}^2 \beta'' A - \frac{3}{2} \bar{n}^3 \alpha'' + \nu_p (\bar{n} - 2)^2 \\ \frac{dc_{gb}}{dt} = \kappa - \frac{dA}{dt} \end{cases} \quad (11)$$

³ In the following, the first and second derivative of the parameters with respect to the cluster size will be indicated, e.g., focusing on the re-solution parameter, as α' and α'' , respectively.

The system is solved considering null initial conditions for all the state variables, implying that all the HBS pores are nucleated during the restructuring process and that they are not interacting with the existing fabrication porosity.

The formulation of the model constituted by Eq. (11) embraces the fundamental physical phenomena governing the gas transfer to the HBS pore under irradiation and during restructuring, i.e., gas diffusion from the interior of the grains, atoms re-solution, and gas atoms trapping. This is in-line with available models conceived for FPC application (e.g., [15]). The novelty of the model we propose in this work lies in the intrinsic consideration of the effects brought about by the evolution of the pore-size distribution. In fact, these effects are embedded in the derivatives of the re-solution and trapping parameters through the Fokker-Planck expansion. Albeit not calculating the complete pore-size distribution, the Fokker-Planck expansion is known to be a satisfactory approximation when the cluster size is large [51] – which is the case of developed HBS porosity. Moreover, the presented model allows for tracking the evolution of the distribution mean size and variance, thus one can assume a certain shape of the pore-size distribution (e.g., log-normal [2]) and compute the evolution of the distribution under irradiation. This feature results in a unique capability offered by the present model for HBS modeling in FPCs, and was proved to be a necessary condition for the correct estimation of HBS pore fracturing under LOCA conditions [34]. Finally, it is worth underlying that the second-order Fokker-Planck expansion (Eq. (10)) of the coefficients retains its validity when the pore-size distribution is sufficiently peaked around the mean value. From the experimental observations available in the open literature [2,52], we can deduce that this condition is met up to around 175 MWd kg_U⁻¹. Beyond this limit, the distributions start to exhibit a wider/multi-modal shape, which would call for high-order expansions or consideration of multiple collisions (e.g. see [26]).

2.2. Pore size calculation

HBS pores are strongly over-pressurized [4,53,54], mainly because of the substantial inflow of fission gas atoms coming from the depleted HBS grains. Thus, they will tend to relieve the pressure by absorbing vacancies by the surrounding medium. A consistent treatment of the vacancy absorption mechanism would require extending the master equations exposed above to a two reacting species CD model. This extension – which is pursued in other fields or by dedicated CD tools [39,51] – would hinder the applicability of the Fokker-Planck procedure exposed above, calling for a multidimensional Fokker-Planck expansion which would increase the computational burden significantly. Thus, we chose to model the vacancy absorption as if it was governed by the mean size of the distribution, rather than consider it, class by class, in the master equations. This is in turn affecting the moments calculation, since the average pore radius is needed in Eqs. (10)–(11) and depends on the number of vacancies calculated as outlined below. Albeit simplified, the developed approach allows estimating the vacancy absorption in a physically grounded manner and with a level of complexity in line with the single size model described by Eq. (11).

As discussed above, we assume HBS pores to be spherical. The pressure of a pore of radius R_n^p (m) obeys the following capillarity relationship

$$p_{eq}^p = \frac{2\gamma}{R_n^p} - \sigma_h \quad (12)$$

where p_{eq}^p (Pa) is the equilibrium pressure, γ (J m⁻²) is the surface energy, and σ_h (Pa) is the hydrostatic stress (considered negative if the medium is under compression). Since pores are, in general, not at equilibrium, they tend to equilibrate by absorbing or emitting

vacancies. The rate of variation of the pore volume is defined via

$$\frac{dV_n^p}{dt} = \omega \frac{d\tilde{n}}{dt} + \Omega \frac{dn_{vp}}{dt} \quad (13)$$

where V_n^p (m^3) is the pore volume, n_{vp} (/) is the number of vacancies per pore, ω (m^3) is the atomic volume for xenon, and Ω (m^3) is the vacancy volume. The content of gas atoms is calculated solving Eq. (11), whereas the vacancy absorption/emission rate dn_{vp}/dt is calculated as [55]

$$\frac{dn_{vp}}{dt} = \frac{2\pi D_{gb}^v \rho_p}{k_B T \zeta} (p^p - p_{eq}^p) \quad (14)$$

where D_{gb}^v ($\text{m}^2 \text{ s}^{-1}$) the vacancy diffusion coefficient at grain boundaries, ρ_p (m) is the radius of the Wigner-Seitz cell⁴ assigned to each pore, k_B (JK^{-1}) is the Boltzmann constant, T (K) is the local temperature, and ζ (/) is a dimensionless factor calculated as

$$\zeta = \frac{10\psi(1 + \psi^3)}{-\psi^6 + 5\psi^2 - 9\psi + 5} \quad (15)$$

where $\psi = R_n^p/\rho_p$ is the ratio between the radii of the pore and of the cell. This factor, which is calculated based on purely geometrical considerations, embodies the effects of the pore radius and pore number density on the vacancy precipitation rate in a spherical object. The original factor was introduced by Speight and Beere [56] to account for a bi-dimensional sink at the grain boundaries, and it was extended to three-dimensional objects by some of the authors in [57,58].

To evaluate the pore pressure, we employ the Hard Spheres (HS) Equation of State (EoS) as proposed by Carnahan and Starling [59], namely

$$\frac{p^p V_n^p}{\tilde{n} k_B T} = \frac{1 + \tilde{y} + \tilde{y}^2 - \tilde{y}^3}{(1 - \tilde{y})^3} \quad (16)$$

The packing fraction, \tilde{y} , is calculated as $\tilde{y} = \pi/6(\delta_{HS}^3 \nu)$ (/) where ν (atom m^{-3}) is the atomic density in the pore and δ_{HS} is Xe HS diameter. The latter is calculated according to Brearley and MacInnes [60], considering a modified Buckingham interatomic potential and reading

$$\delta_{HS} = 4.45 \cdot 10^{-10} \left(0.8542 - 0.03996 \cdot \log \left(\frac{T}{231.2} \right) \right) \quad (17)$$

with the local temperature, T , expressed in K. This expression is used, combined to the definition of \tilde{y} , to evaluate the volume occupied by each gas atom in the pore, namely $\omega = \tilde{y}/\nu$.

The pore growth due to vacancy and gas atom absorption may trigger another mechanism of growth, i.e., interconnection by impingement. The treatment of interconnection is based on [58] and reads

$$\frac{dN_p}{dV_p} = -4\lambda^p N_p^2 \quad (18)$$

where $\lambda^p = (2 - \xi)/[2(1 - \xi)^3]$ is a correction factor limiting the interconnection rate when high local porosity is achieved and accounting for the non-superposition of hard spheres. A more rigorous treatment of the interconnection between polydispersed pores would entail the inclusion of additional, non-linear terms in the cluster dynamics master equations (Eq. (1)), as shown e.g. in [38]. Nevertheless, this inclusion would require the solution of the overall system of equations and would invalidate the Fokker-Planck expansion. Indeed, the solution of the cluster dynamics master equations is not feasible for application to FPCs of the present model,

Table 1

Expressions of the model parameters.

Parameter	Expression/Value	Reference
D_{gb}^{SA}	$D_{gb}^{SA} = 1.3 \cdot 10^{-7} \exp(-4.52 \cdot 10^{-19}/k_B T)$	[61]
D_{gb}^v	$D_{gb}^v = 8.86 \cdot 10^{-6} \exp(-5.75 \cdot 10^{-19}/k_B T) + 10^{-39} \dot{f}$	[62,63]
ν_p	$\nu_p = 5 \cdot 10^{17} d\alpha_r/dbu_{eff}$	This work
d_v	$d_v = 1 \text{ nm}$	[40]
δ_v	$\delta_v = 1 \text{ nm}$	[40]
γ	$\gamma = 1 \text{ J m}^{-2}$	[35]
Ω	$\Omega = 4.09 \cdot 10^{-29} \text{ m}^3$	[35]

thus we decided to consider the interconnection as it would happen among monodispersed spheres featured by the average radius of the distribution.

The model presented in this Section allows for a reasonable description of the evolution of HBS porosity and presents various original contributions with respect to the state of the art. First, the foundation of the modeling approach lies on the master equations of cluster dynamics. This allows for consideration of the effects due to the pore size distribution on the trapping and resolution rates, constituting a step forward with respect to the available single-size models [10,13,15,19,24]. Second, the introduction of the dependence of grain boundary diffusivity on the tilt angle of grain boundaries physically embodies a feature often introduced artificially in HBS porosity modeling (e.g., [10,15]) to reproduce experimental data. Third, the developed approach allows for tracking the evolution under irradiation of the pore-size distribution mean and variance. These figures, combined with the assumption of a pore-size distribution *a priori* known, enables a consistent calculation of the evolution of the pore-size distribution under irradiation. Thus, the model can be plugged upon mechanistic models which need as input the distribution of HBS pore pressures to estimate micromechanics phenomena, such as grain boundary loss of cohesion in accident transients [34].

3. Results and discussion

The presented results were obtained implementing the model into the SCIANTIX code [32]. We showcase the capability of the model to account for matrix (macroscopic) swelling modification as HBS formation occurs. Lastly, we compare the predictions of the model for the porosity evolution to recent experimental data, in terms of pore number density, mean radius, and the resulting gaseous swelling.

3.1. Choice of model parameters

The expressions of parameters employed in SCIANTIX are reported in Table 1, and discussed in this Section. For those concerning the intra-granular behavior and HBS formation model, the reader should refer to the companion paper [29].

For the grain boundary diffusivity of fission gas, the correlation (denoted as “low D”) proposed by Olander and Van Uffelen [61] is employed, as it is one of the few available correlations for this parameter in the open literature. The diffusion coefficient of vacancies along the grain boundaries is accounted for through an expression complementing the coefficient proposed by White [63] with an a-thermal factor, as suggested by Matzke [62] and as considered also by Jernkvist [6]. This latter parameter is as uncertain as the diffusion coefficient of gas atoms along the grain boundaries, being normally extracted from diffusional creep measurements. It represents an important parameter, governing the kinetics of pore growth, but it must be underlined that it does not determine the asymptotic size of the pores. In fact, it affects only the kinetic of their evolution (cfr Eq. (14)). The re-resolution

⁴ The radius of the Wigner-Seitz cell is determined from the relationship $\frac{4}{3}\pi N_p \rho_p^3 = 1$. A sketch of the system is reported in Fig. 1a.

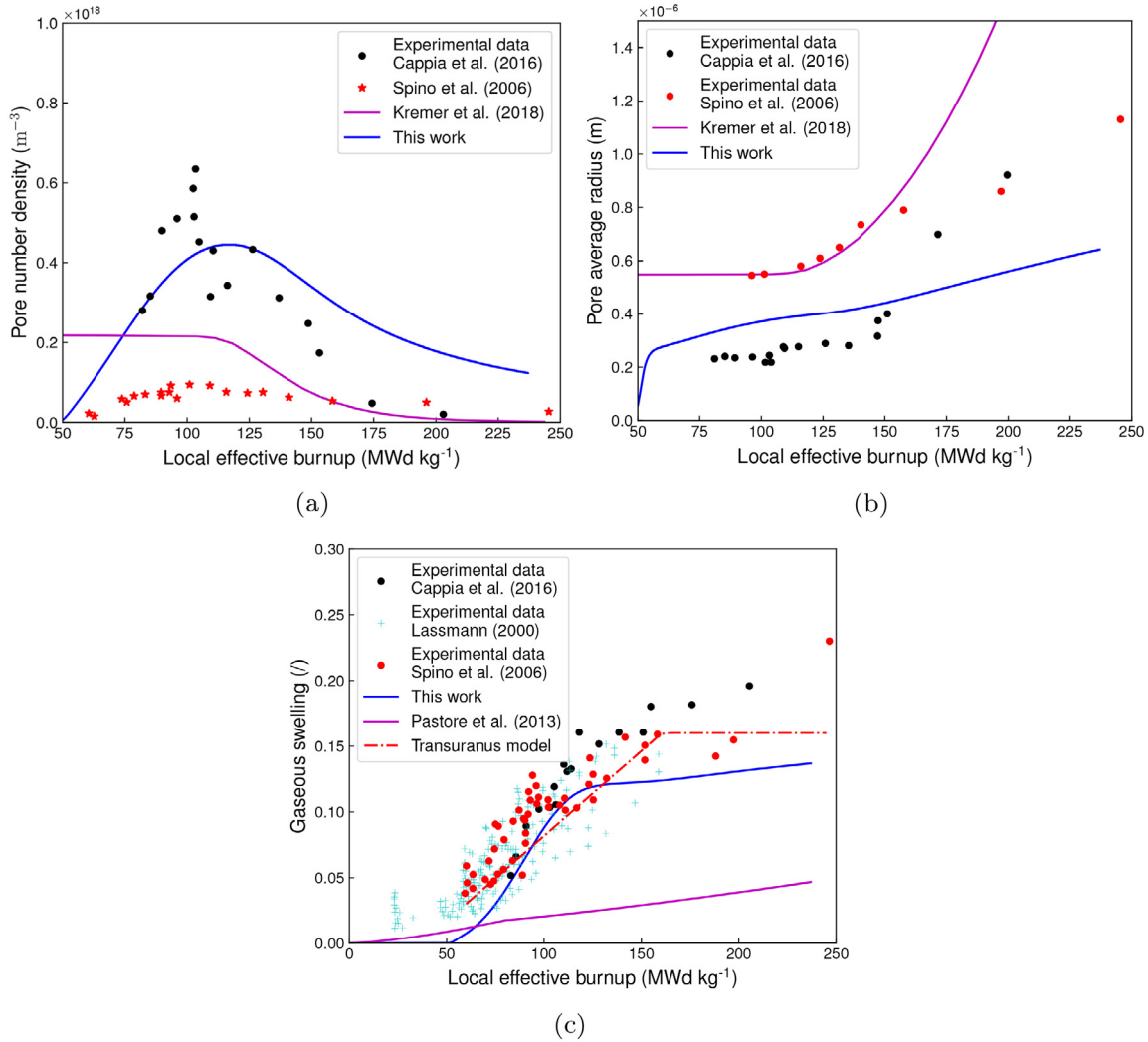


Fig. 2. Comparison of experimental data on HBS pore number density, number-averaged radius, and gaseous swelling (i.e., on local porosity) taken from Cappia and co-workers [2,52], Spino and co-workers [1], and from Vennix as reported by Lassmann [66] to model predictions. For the sake of comparison, we include the predictions of state-of-the-art models, namely the model proposed by Kremer and coworkers [18], the correlation-based model of TRANSURANUS accounting for HBS porosity [66], and the mechanistic model by Pastore et al. [67] accounting for gaseous swelling in low-medium burnup conditions.

of the HBS inter-granular pores is accounted for following the model by Veshchunov and Tarasov [40]. In fact, the model by Turnbull would predict an indefinite increase of re-resolution probability with the bubble size, while recent lower length scale calculations demonstrate an attenuation of re-resolution with increasing bubble radii [64].

Lastly, the nucleation rate of HBS pores is evaluated as a constant value, proportional to the variation of the local degree of restructuring. Indeed, this approach reflects the experimental findings [1–3] but calls for a future, mechanistic refinement, that could involve the description of point defects like in the MFPR/F and MFPR/R codes.

3.2. HBS porosity

In Figs. 2(a)–2(c), we compare the model predictions in terms of pore number density, mean radius, and resulting gaseous swelling as a function of local effective burnup⁵ to the recent experimen-

tal data on HBS porosity in UO₂ obtained by Cappia and co-workers [2,52], as well as to experimental data from Spino and co-workers [1]. The results presented by Kremer and coauthors [18] using the MFPR/F code on the same data-set are included for the sake of comparison. We underline that the experimental data considered in this work were obtained using different experimental techniques, namely, optical or electronic microscopy, and different methods to address the stereology of the problem (i.e., to pass from 2D to 3D configurations). It must be underlined that the combinations of these latter aspects have a non-negligible impact on the data extraction [2,52] and that a definitive conclusion on the correct path is not yet available in the open literature. Thus, we consider in this analysis all of the available experimental data without deeming one dataset superior to the other.

⁵ Holt and coauthors [65], reading

$$bu_{eff} = \int H(T - \bar{T}) dbu \quad (19)$$

where $H(\bar{T})$ is the Heaviside function, T (°C) the local temperature, and \bar{T} is a threshold temperature taken equal to 1000 °C.

⁵ The effective burnup is a quantity introduced by Khvostov [12] to account for the accumulation of irradiation damage at temperatures low enough to prevent the annealing of defects. We chose the definition of effective burnup as proposed by

The calculated quantities have been obtained considering an irradiation history representative for the conditions met in the periphery of a fuel pellet in PWRs, namely, a temperature of 723 K, a fission rate density equal to $2 \cdot 10^{19}$ fissions $\text{m}^{-3} \text{s}^{-1}$, and a hydrostatic stress equal to 20 MPa representative for pellet-cladding mechanical interaction. The considered experimental databases, taken from Lassmann [66], Spino and coworkers [1], and Cappia and coworkers [2,52], consist of samples coming from a homogeneous set of material composition (i.e., uranium dioxide) and irradiation (i.e., commercial LWRs). Note that the comparisons only account for the burnup because no other details of the specific irradiation histories are accessible in the open literature. Despite this limitation, we propose these comparisons to provide an indication of the model ability to represent the dependence of HBS porosity on the local burnup observed experimentally.

Considering the uncertainty of model parameters and the modeling approach which must ensure a compatibility with the speed of computation required for FPCs, as well as the dispersion of the experimental data, the agreement between the predicted results and the experimental results is deemed encouraging. As a general trend, the agreement between the calculated quantities and the experimental data is very satisfying until 130 MWd $\text{kg}_{\text{U}}^{-1}$, whereas above this value higher discrepancies arise. In particular, the overestimation of pore number density and underestimation of pore average radius beyond 150 MWd $\text{kg}_{\text{U}}^{-1}$ (Figs. 2a and 2b) suggest that the growth of the HBS pores might be somehow underestimated at ultra high burnups. In particular, the slope of the calculated pore radius as a function of effective burnup does increase around this burnup value, while such an increase is apparent in the experimental data (Fig. 2 b). The results obtained by Kremer et al. [18], on the other hand, showcase larger radii and lower number densities. It must be underlined that these results are obtained fixing a constant porosity (in this case, equal to 15%) and considering an empirical fit of the pore radii as a function of burnup, then evaluating pore number density as a consequence. The results show that the radii calculated by Kremer et al. [18] are indeed larger, yet such an outcome results from a purely empirical correlation. As for the resulting gaseous swelling, the experimental data are generally underestimated, with the discrepancies increasing for the pore evolution at ultra-high burnups.

Indeed, the step forward brought about by the present modeling approach is apparent in Fig. 2c, where we compare the predictions of the proposed model to models included in state-of-the-art FPCs accounting for gaseous swelling and/or HBS pore swelling. The predictions by the MFPPF/F code are not included since the swelling is an input parameter of the model and in this case would be a constant value at 15%. In particular, the comparison includes the correlation-based model available in TRANSURANUS to account for HBS porosity [66] and the mechanistic model by Pastore and co-workers [67], which accounts for gaseous swelling in unrestructured fuel. Although the latter model is not conceived for HBS, the comparison highlights the importance of a dedicated model for the HBS porosity description as the one developed in this work. As for the former model, available in the TRANSURANUS code, it was derived as a pure fit of experimental data of porosity as a function of local burnup, and its predictions are in-line with those obtained by the newly developed, physics based model. Experimental data used to draw the TRANSURANUS empirical correlation, obtained by Vennix and reported in [66], are included for the sake of comparison. In the light of these promising results, the presented model has been made available to the TRANSURANUS code users via a coupling scheme with SCIENTIX. The coupled code suite will be subsequently validated against integral irradiation experiments including high burnup rods, to assess the impact of the HBS porosity model on the overall fuel rod performance.

4. Conclusions

In this work, we presented a model for the HBS porosity evolution, based on a Fokker-Planck expansion of the cluster dynamics master equations describing the pore behavior at grain boundaries. The Fokker-Planck approximation is truncated at the second order, yielding a model featured by a limited number of equations – thus, applicable to engineering fuel performance calculations – yet allows the estimation of the evolution of pore number density, mean size and variance of the pore size distribution. In this framework, the pore evolution model considers, in a physically-based manner, the phenomena determining the pore size, i.e., fission gas absorption, gas atoms re-solution, vacancy absorption to compensate for pore over-pressurization, and pore interconnection. The consideration of the HBS pore size distribution also paves the way to model fuel fragmentation in high burnup fuel [34].

The comparisons of model calculations to experimental data on HBS porosity shows a satisfactory agreement in terms of pore number density and average radius. Albeit slightly underestimating the resulting gaseous swelling, the model ensures a substantial step forward with respect to state-of-the-art models available in fuel performance codes for the estimation of HBS porosity. The present work will be complemented in the future by an integral assessment of the overall model on fuel performance simulations, namely via the TRANSURANUS-SCIENTIX code suite, of high burnup rods.

The underestimated pore growth at ultra high burnups calls for additional modeling efforts. A possible development path could entail the consideration of higher order pore interactions during the interconnection process, as made by Veshchunov and co-workers [25,26] introducing a three-body scheme, or considering the interaction of a population of polydispersed spheres in the two-body scheme. Finally, we underline that a set of substantial uncertainties on both model parameters and irradiation conditions exist. To this point, a sensitivity analysis to model parameters affected by the largest uncertainties, such as the grain boundary diffusion coefficient of gas atoms, its correction as a function of the tilt angle, and the restructuring and nucleation rates, would help to shed light on the potential impact of these uncertainties on the model predictions. Similarly, input quantities for the calculations, such as local fission rate, temperature, and hydrostatic stress are affected by significant uncertainties, whose impact on the results needs to be assessed by such analysis.

Declaration of Competing Interest

The authors declare that they have no known competing financial interests or personal relationships that could have appeared to influence the work reported in this paper.

CRediT authorship contribution statement

Tommaso Barani: Conceptualization, Methodology, Software, Validation, Writing – original draft, Visualization. **Davide Pizzocri:** Conceptualization, Methodology, Writing – review & editing. **Fabiola Cappia:** Conceptualization, Data curation, Writing – review & editing. **Giovanni Pastore:** Writing – review & editing, Supervision. **Lelio Luzzi:** Writing – review & editing, Funding acquisition, Supervision. **Paul Van Uffelen:** Conceptualization, Methodology, Software, Data curation, Writing – original draft, Funding acquisition, Supervision.

Acknowledgments

This work has been supported by the ENEN + project that has received funding from the Euratom research and training Work

Programme 2016–2017-1 #755576, and has received funding from the Euratom research and training programme 2014–2018 through the INSPYRE Project under grant agreement No. 754329.

This work contributes to the U.S.-EURATOM International Nuclear Energy Research Initiative (INERI) project 2017-004-E on Modelling of Fission Gas Behaviour in Uranium Oxide Nuclear Fuel Applied to Engineering Fuel Performance Codes.

The submitted manuscript has been authored by a contractor of the U.S. Government under Contract DE-AC07-05ID14517. Accordingly, the U.S. Government retains a non-exclusive, royalty free license to publish or reproduce the published form of this contribution, or allow others to do so, for U.S. Government purposes.

References

- [1] J. Spino, A.D. Stalios, H. Santa Cruz, D. Baron, Stereological evolution of the rim structure in PWR-fuels at prolonged irradiation: dependencies with burn-up and temperature, *J. Nucl. Mater.* 354 (1–3) (2006) 66–84.
- [2] F. Cappia, D. Pizzocri, A. Schubert, P. Van Uffelen, G. Paperini, D. Pellottier, R. Macian-Juan, V.V. Rondinella, Critical assessment of the pore size distribution in the rim region of high burnup UO_2 fuels, *J. Nucl. Mater.* 480 (2016) 138–149.
- [3] C. Walker, Assessment of the radial extent and completion of recrystallisation in high burn-up UO_2 nuclear fuel by EPMA, *J. Nucl. Mater.* 275 (1) (1999) 56–62.
- [4] J. Noirot, L. Desgranges, J. Lamontagne, Detailed characterisations of high burn-up structures in oxide fuels, *J. Nucl. Mater.* 372 (2–3) (2008) 318–339.
- [5] F. Lemoine, D. Baron, P. Blanpain, Key parameters for the High Burnup Structure formation thresholds, 2010 LWR Fuel Performance Meeting/Top Fuel/WRFP, 2010, Orlando, Florida, USA.
- [6] L.O. Jernkvist, Modelling of fine fragmentation and fission gas release of UO_2 fuel in accident conditions, *EPJ Nuclear Sci. Technol.* 5 (2019) 11.
- [7] K. Lassmann, C. Walker, J. van de Laar, F. Lindström, Modelling the high burnup UO_2 structure in LWR fuel, *J. Nucl. Mater.* 226 (1995) 1–8.
- [8] K. Geelhood, W. Luscher, P. Raynaud, I. Porter, FRAPCON-4.0: a Computer Code for the Calculation of Steady-state, Thermal-Mechanical Behavior of Oxide Fuel Rods for High Burnup, Technical Report, 2015.
- [9] M. Lemes, A. Soba, A. Denis, An empirical formulation to describe the evolution of the high burnup structure, *J. Nucl. Mater.* 456 (2015) 174–181.
- [10] P. Blair, A. Romano, C. Hellwig, R. Chawla, Calculations on fission gas behaviour in the high burnup structure, *J. Nucl. Mater.* 350 (3) (2006) 232–239.
- [11] A. Denis, A. Soba, Simulation of pellet-cladding thermomechanical interaction and fission gas release, *Nucl. Eng. Des.* 223 (2) (2003) 211–229.
- [12] G. Khvostov, V. Novikov, A. Medvedev, S. Bogaty, Approaches to Modeling of high burn-up structure and analysis of its effects on the behaviour of light water reactor fuels in the START-3 fuel performance code, Water Reactor Fuel Performance Meeting/WRFP, 2005, 2005.
- [13] G. Khvostov, K. Mikityuk, M.A. Zimmermann, A model for fission gas release and gaseous swelling of the uranium dioxide fuel coupled with the FALCON code, *Nucl. Eng. Des.* 241 (8) (2011) 2983–3007.
- [14] Y. Rashid, R. Dunham, R. Montgomery, Fuel analysis and licensing code: FALCON MOD01 volume 1: theoretical and numerical bases 1 (3) (2004) 246.
- [15] L. Noirot, MARGARET: A comprehensive code for the description of fission gas behavior, *Nucl. Eng. Des.* 241 (6) (2011) 2099–2118, doi:10.1016/j.nucengdes.2011.03.044.
- [16] J. Sercombe, I. Aubrun, C. Nonon, Power ramped cladding stresses and strains in 3D simulations with burnup-dependent pellet-clad friction, *Nucl. Eng. Des.* 242 (2012) 164–181.
- [17] B. Baurens, J. Sercombe, C. Riglet-Martial, L. Desgranges, L. Trotignon, P. Maugis, 3D thermo-chemical-mechanical simulation of power ramps with ALCYONE fuel code, *J. Nucl. Mater.* 452 (1–3) (2014) 578–594.
- [18] F. Kremer, R. Dubourg, F. Cappia, V. Rondinella, A. Schubert, P. Van Uffelen, T. Wiss, High Burn Up Structure formation and growth and fission product release modelling: new simulations in the mechanistic code MFPR-F, in: TopFuel 2018, Prague, Czech Republic, 2018, pp. 1–12.
- [19] J. Rest, The effect of irradiation-induced gas-atom re-solution on grain-boundary bubble growth, *J. Nucl. Mater.* 321 (2–3) (2003) 305–312, doi:10.1016/S0022-3115(03)00303-9.
- [20] J. Rest, A model for the influence of microstructure, precipitate pinning and fission gas behavior on irradiation-induced recrystallization of nuclear fuels, *J. Nucl. Mater.* 326 (2) (2004) 175–184.
- [21] M.S. Veshchunov, V.E. Shestak, Model for evolution of crystal defects in UO_2 under irradiation up to high burn-ups, *J. Nucl. Mater.* 384 (2009) 12–18, doi:10.1016/j.jnucmat.2008.09.024.
- [22] K. Nogita, K. Une, Irradiation-induced recrystallization in high burnup UO_2 fuel, *J. Nucl. Mater.* 226 (3) (1995) 302–310.
- [23] U. Gösele, Concentration dependence of rate constants for diffusion- or reaction-controlled void-point-defect reactions, *J. Nucl. Mater.* 78 (1) (1978) 83–95, doi:10.1016/0022-3115(78)90507-X.
- [24] V.I. Tarasov, M.S. Veshchunov, Models for fuel porosity evolution in UO_2 under various regimes of reactor operation, *Nucl. Eng. Des.* 272 (2014) 65–83, doi:10.1016/j.nucengdes.2014.02.016.
- [25] M.S. Veshchunov, V.I. Tarasov, Modelling of pore coarsening in the high burn-up structure of UO_2 fuel, *J. Nucl. Mater.* 488 (2017) 191–195, doi:10.1016/j.jnucmat.2017.03.013.
- [26] V.I. Tarasov, P.V. Polovnikov, V.E. Shestak, M.S. Veshchunov, Development of the MFPR/R code for characterization of the rim zone and high burnup structure evolution in UO_2 fuel pellets, *J. Nucl. Mater.* 517 (2019) 214–224, doi:10.1016/j.jnucmat.2019.01.055.
- [27] M.S. Veshchunov, V.D. Ozrin, V.E. Shestak, V.I. Tarasov, R. Dubourg, G. Nicaise, Development of the mechanistic code MFPR for modelling fission-product release from irradiated UO_2 fuel, *Nucl. Eng. Des.* 236 (2) (2006) 179–200, doi:10.1016/j.nucengdes.2005.08.006.
- [28] M. Veshchunov, A. Boldyrev, A. Kuznetsov, V. Ozrin, M. Seryi, V. Shestak, V. Tarasov, G. Norman, A. Kuksin, V. Pisarev, D. Smirnova, S. Starikov, V. Stegailov, A. Yanilkin, Development of the advanced mechanistic fuel performance and safety code using the multi-scale approach, *Nucl. Eng. Des.* 295 (2015) 116–126, doi:10.1016/j.nucengdes.2015.09.035.
- [29] T. Barani, D. Pizzocri, F. Cappia, L. Luzzi, G. Pastore, P.V. Uffelen, Modeling high burnup structure in oxide fuels for application to fuel performance codes. part I: high burnup structure formation, *J. Nucl. Mater.* 539 (2020) 152296.
- [30] A. Kolmogorov, On the statistical theory of metal crystallization, *Izv. Akad. Nauk SSSR, Ser. Math.* (1937) 335–360.
- [31] M. Kinoshita, Mesoscopic approach to describe high burn-up fuel behaviour, Enlarged HPG Meeting on High Burn-up Fuel Performance, Safety and Reliability and Degradation of In-core Materials and Water Chemistry Effects and Man-machine Systems Research, Loen (Norway), 24–29 May, 1999.
- [32] D. Pizzocri, T. Barani, L. Luzzi, SCIENTIX: A new open source multi-scale code for fission gas behaviour modelling designed for nuclear fuel performance codes, *J. Nucl. Mater.* 532 (2020) 152042, doi:10.1016/j.jnucmat.2020.152042.
- [33] K. Lassmann, TRANSURANUS: A fuel rod analysis code ready for use, *J. Nucl. Mater.* 188 (1992) 295–302.
- [34] K. Kulacsy, Mechanistic model for the fragmentation of the high-burnup structure during LOCA, *J. Nucl. Mater.* 466 (2015) 409–416, doi:10.1016/j.jnucmat.2015.08.015.
- [35] T. Kogai, Modelling of fission gas release and gaseous swelling of light water reactor fuels, *J. Nucl. Mater.* 244 (1997) 131–140, doi:10.1016/S0022-3115(96)00731-3.
- [36] P. Van Uffelen, Contribution to the modelling of fission gas release in Light Water Reactor fuel, Université de Liège, 2002 Ph.D. thesis.
- [37] C.F. Clement, M.H. Wood, Equations for the growth of a distribution of small physical objects, *Proc. R. Soc. London A368* (1979) 521.
- [38] M. Fell, S.M. Murphy, The nucleation and growth of gas bubbles in irradiated metals, *J. Nucl. Mater.* 172 (1990) 1–12.
- [39] T. Jourdan, G. Bencteux, G. Adjanor, Efficient simulation of kinetics of radiation induced defects: a cluster dynamics approach, *J. Nucl. Mater.* 444 (1–3) (2014) 298–313.
- [40] M.S. Veshchunov, V.I. Tarasov, Modelling of irradiated UO_2 fuel behaviour under transient conditions, *J. Nucl. Mater.* 437 (1–3) (2013) 250–260, doi:10.1016/j.jnucmat.2013.02.011.
- [41] F. Ham, Theory of diffusion-limited precipitation, *J. Phys. Chem. Solids* 6 (1958) 335–351.
- [42] M.S. Veshchunov, On the theory of fission gas bubble evolution in irradiated UO_2 fuel, *J. Nucl. Mater.* 277 (2000) 67–81.
- [43] D.R. Olander, D. Wongsawaeng, Re-solution of fission gas - A review: part i. intragranular bubbles, *J. Nucl. Mater.* 354 (1–3) (2006) 94–109, doi:10.1016/j.jnucmat.2006.03.010.
- [44] T.J. Gerczak, C.M. Parish, P.D. Edmondson, C.A. Baldwin, K.A. Terrani, Restructuring in high burnup UO_2 studied using modern electron microscopy 509 (2018) 245–259.
- [45] J. Noirot, I. Zacharie-Aubrun, T. Blay, Focused ion beam/scanning electron microscope examination of high burn-up UO_2 in the center of a pellet, *Nuclear Engineering and Technology* 50 (2) (2018) 259–267.
- [46] K. Nogita, K. Une, Radiation-induced microstructural change in high burnup UO_2 fuel pellets, *Nucl. Instrum. Methods Phys. Res., Sect. B* 91 (1994) 301–306.
- [47] M. Kinoshita, Towards the mathematical model of rim structure formation, *J. Nucl. Mater.* 248 (1997) 185–190.
- [48] K. Nogita, K. Une, M. Hirai, K. Ito, K. Ito, Y. Shirai, Effect of grain size on recrystallization in high burnup fuel pellets, *J. Nucl. Mater.* 248 (1997) 196–203.
- [49] N.L. Peterson, Diffusion mechanisms and structural effects in grain boundaries, *Journal of Vacuum Science & Technology A: Vacuum, Surfaces, and Films* 4 (6) (1986) 3066–3070, doi:10.1116/1.573629.
- [50] D. Baron, B. Hermitte, J. Piron, An attempt to simulate the porosity buildup in the rim at high burnup, IAEA Technical Committee Meeting on Advances in Fuel Pellet Technology for Improved Performance at High Burnup, 1996, Tokyo, Japan.
- [51] A.A. Kohnert, B.D. Wirth, L. Capolungo, Modeling microstructural evolution in irradiated materials with cluster dynamics methods: a review, *Comput. Mater. Sci.* 149 (2018) 442–459.
- [52] F. Cappia, Investigation of very high burnup UO_2 fuels in Light Water Reactors, Technischen Universität München, 2017 Ph.D. thesis.
- [53] C. Walker, S. Bremier, S. Portier, R. Hasnaoui, W. Goll, SIMS Analysis of an UO_2 fuel irradiated at low temperature to 65 MWd/kgHM, *J. Nucl. Mater.* 393 (2) (2009) 212–223.
- [54] J. Noirot, J. Lamontagne, N. Nakae, T. Kitagawa, Y. Kosaka, T. Tverberg, Heterogeneous UO_2 fuel irradiated up to a high burn-up: investigation of the HBS and of fission product releases, *J. Nucl. Mater.* 442 (1–3) (2013) 309–319.

- [55] M. Speight, W. Beere, Vacancy potential and void growth on grain boundaries, *Met. Sci.* 9 (1975) 190–191.
- [56] M.V. Speight, W. Beere, Vacancy potential and void growth on grain boundaries, *Metal Science* 9 (1975) 190–191.
- [57] T. Barani, G. Pastore, D. Pizzocri, D.A. Andersson, C. Matthews, A. Alfonsi, K.A. Gamble, P. Van Uffelen, L. Luzzi, J.D. Hales, Multiscale modeling of fission gas behavior in U_3Si_2 under LWR conditions, *J. Nucl. Mater.* 522 (2019) 97–110, doi:[10.1016/j.jnucmat.2019.04.037](https://doi.org/10.1016/j.jnucmat.2019.04.037).
- [58] T. Barani, G. Pastore, A. Magni, D. Pizzocri, P.V. Uffelen, L. Luzzi, Modeling intra-granular fission gas bubble evolution and coarsening in uranium dioxide during in-pile transients, *J. Nucl. Mater.* 538 (2020) 152195.
- [59] N.F. Carnahan, K.E. Starling, Equation of state for nonattracting rigid spheres, *J Chem Phys* 51 (2) (1969) 635–636, doi:[10.1063/1.1672048](https://doi.org/10.1063/1.1672048).
- [60] I.R. Brearley, D.A. MacInnes, An improved equation of state for inert gases at high pressures, *J. Nucl. Mater.* 95 (3) (1980) 239–252, doi:[10.1016/0022-3115\(80\)90365-7](https://doi.org/10.1016/0022-3115(80)90365-7).
- [61] D. Olander, P. Van Uffelen, On the role of grain boundary diffusion in fission gas release, *J. Nucl. Mater.* 288 (2–3) (2001) 137–147, doi:[10.1016/S0022-3115\(00\)00725-X](https://doi.org/10.1016/S0022-3115(00)00725-X).
- [62] H.J. Matzke, Atomic transport properties in UO_2 and mixed oxides (U,Pu) O_2 , *J. Chem. Soc., Faraday Trans. 2* 83 (1987) 1121–1142.
- [63] R.J. White, The development of grain-face porosity in irradiated oxide fuel, *J. Nucl. Mater.* 325 (1) (2004) 61–77, doi:[10.1016/j.jnucmat.2003.10.008](https://doi.org/10.1016/j.jnucmat.2003.10.008).
- [64] W. Setyawan, M.W. Cooper, K.J. Roche, R.J. Kurtz, B.P. Uberuaga, D.A. Andersson, B.D. Wirth, Atomistic model of xenon gas bubble re-resolution rate due to thermal spike in uranium oxide, *J Appl Phys* 124 (7) (2018), doi:[10.1063/1.5042770](https://doi.org/10.1063/1.5042770).
- [65] L. Holt, A. Schubert, P. Van Uffelen, C.T. Walker, E. Fridman, T. Sonoda, Sensitivity study on Xe depletion in the high burn-up structure of UO_2 , *J. Nucl. Mater.* 452 (1–3) (2014) 166–172.
- [66] K. Lassmann, A. Schubert, J. van de Laar, C. Vennix, Developments of the TRANSURANUS code with emphasis on high burnup phenomena, IAEA Technical Committee Meeting on Nuclear Fuel Behaviour Modelling at High Burnup, 2000, Lake Windermere, U.K.
- [67] G. Pastore, L. Luzzi, V. Di Marcello, P. Van Uffelen, Physics-based modelling of fission gas swelling and release in UO_2 applied to integral fuel rod analysis, *Nucl. Eng. Des.* 256 (2013) 75–86, doi:[10.1016/j.nucengdes.2012.12.002](https://doi.org/10.1016/j.nucengdes.2012.12.002).